Lipid Bilayer Perturbations Induced by Simple Hydrophobic Peptides†

Russell E. Jacobs* and Stephen H. White

Department of Physiology & Biophysics, University of California, Irvine, Irvine, California 92717

Received December 10, 1986; Revised Manuscript Received May 18, 1987

ABSTRACT: Mixtures of tripeptides of the form Ala-X-Ala-*O-tert*-butyl with 1,2-dimyristoyl-*sn*-glycero-3-phosphocholine (DMPC) bilayers have been used as a model system for studying the influence of hydrophobic peptides on membrane order and dynamic properties by means of deuterium NMR spectroscopy. Tripeptides with X = Ala, Leu, Phe, and Trp have been examined. Lipid ^2H NMR spectra of acyl chain perdeuteriated DMPC ([$^2H_{54}$]DMPC) show that the addition of peptide disorders the bilayer lipid acyl chains and that the extent of the perturbation increases as the size of the central residue increases. Moment analyses of the spectra indicate that, while the average acyl chain order parameter *decreases* with increasing central residue size, the order parameter spread across the bilayer (the mean-squared width of the distribution) *increases*. Lipid segmental ^2H longitudinal relaxation rates, $1/T_1(i)$, exhibit a square-law functional dependence on $S_{CD}(i)$ both with and without the addition of peptide. The addition of peptide causes an increase in the *slope* of plots of $1/T_1(i)$ vs. $|S_{CD}(i)|^2$ with little change in the $1/T_1(i)$ intercept, indicating a complex modulation of the acyl chain motions. ^2H NMR spectra of Ala-[$^2H_4$]Ala-Ala-*O-tert*-butyl in DMPC bilayers have both isotropic and powder pattern components that vary as a function of temperature. At 30 °C the ^2H spin–lattice relaxation times for the labeled Ala residue increase in going from bilayer-incorporated peptide to polycrystalline peptide to polycrystalline Ala·HCl. These experiments provide no information on the location of these peptides in the bilayer. If they protrude into the hydrocarbon core, their disordering influence can be attributed to a direct disruption of acyl chain packing. If they are adsorbed to the bilayer surface, their influence on the bilayer interior must be an indirect disruption propagated via the head group region.

The lipid bilayer is the basic structural unit of the cell membrane within which proteins carry out the enzymatic and other tasks associated with membrane function. The issues surrounding the interplay between these components are complex and are of fundamental importance to understanding the many activities of cell membranes. Model systems composed of a chemically well-defined lipid bilayer and a single species of peptide or protein are relatively easy to manipulate and can provide insights into the basic interactions of proteins with lipid bilayers. Several physical techniques have been employed in the study of lipid/protein interactions in model systems. Differential scanning calorimetry has been used to examine a large number of systems (Silvius, 1982) including reconstituted enzyme systems [Ca^{2+}-ATPase (Lentz et al., 1985) and cytochrome *c* oxidase (Rigell et al., 1985)], physiologically active peptides (Surewicz & Epand, 1985), and synthetic hydrophobic peptides of different lengths (Morrow et al., 1985). Infrared, Raman, and circular dichroism techniques have been particularly useful in the study of the conformation of membrane-bound peptides (Naik & Krimm, 1986; Gremlich et al., 1983; Wallace et al., 1981; Briggs & Gierasch, 1984), while magnetic resonance (ESR[1] and NMR) and fluorescence spectroscopy have been used to evaluate both static and dynamic properties of lipid/protein interactions (Bell, 1981; Bloom et al., 1986; Smith & Oldfield, 1984; Rehorek et al., 1985; Cornell et al., 1982; Wolber & Hudson, 1982).

In this work we describe ^2H NMR investigations of mixtures formed from a homologous series of hydrophobic tripeptides with lipid bilayers. The tripeptides have the form Ala-X-Ala-*O-tert*-butyl, where X is one of four hydrophobic amino acid residues. The Ala residues serve to put the central "X" residue in a protein-like covalent environment, while the terminal *tert*-butyl group enhances the binding of the molecule to the bilayer. In a previous study we found that peptides of this form alter the characteristics of the lipid bilayer thermal phase transition, that they have water-to-bilayer molar partition coefficients (K_p) ranging from 100 to 5000, depending upon the identity of the central residue, and that the Trp fluorescence properties indicate a partitioning of the Trp-containing peptide into a low dielectric medium (Jacobs & White, 1986). The phase behavior observed previously is faithfully reflected in the lipid ^2H NMR spectra reported here. Spin–lattice relaxation measurements are used to assess how the presence of peptide modulates the dynamic behavior of the lipid acyl chains. Similar measurements using Ala-Ala-Ala-*O-tert*-butyl deuterium labeled in the central Ala residue reveal that the behavior of this peptide in mixtures with DMPC bilayers is quite complex.

Materials and Methods

Isotopically labeled alanine and DMPC were purchased from Cambridge Isotopes, Inc. (Cambridge, MA), unlabeled DMPC from Avanti Polar Lipids (Birmingham, AL), tritiated

† This work was supported by grants from the National Institutes of Health (RR 01993) and the National Science Foundation (DMB-8412754).

* Author to whom correspondence should be addressed.

[1] Abbreviations: NMR, nuclear magnetic resonance; ESR, electron spin resonance; DMPC, 1,2-dimyristoyl-*sn*-glycero-3-phosphocholine; DLPC, 1,2-dilauroyl-*sn*-glycero-3-phosphocholine; DPPC, 1,2-dipalmitoyl-*sn*-glycero-3-phosphocholine; [$^2H_{54}$]DMPC, 1,2-bis(perdeuteriomyristoyl)-*sn*-glycero-3-phosphocholine; A or Ala, alanine; L or Leu, leucine; F or Phe, phenylalanine; W or Trp, tryptophan; $S_{CD}(i)$, C–^2H bond order parameter for the *i*th acyl chain methylene group; DSC, differential scanning calorimetry; Boc, *tert*-butoxycarbonyl.

0006-2960/87/0426-6127$01.50/0

DMPC from New England Nuclear (Boston, MA), and deuterium-depleted water from Sigma Chemical Co. (St. Louis, MO). Peptides were synthesized and purified by standard methods as previously described (Jacobs & White, 1986).

All the NMR samples consisted of lipid/peptide mixture dispersed in excess 50 mM phosphate-buffered deuterium-depleted water. The appropriate amounts of lipid and peptide were first codissolved in chloroform to ensure complete mixing. The solvent was then evaporated under a stream of dry N_2 and the sample placed under high vacuum overnight. After addition of deuterium-depleted buffer the sample tube was sealed and the sample mixed by vortexing and raising and lowering the sample temperature through the lipid bilayer phase transition. All samples used in this study were made up to contain a lipid/peptide mole ratio of 5/1. Using previously determined partition coefficients for the Trp-, Phe-, and Ala-containing peptides (Jacobs & White, 1986) and a value of 911 for the partition coefficient for the Leu-containing peptide (R. E. Jacobs and S. H. White, unpublished results) we calculate the following amounts of peptide actually associated with the bilayer: Trp, 98%; Phe, 93%; Leu, 91%; and Ala, 65%. Although it should be noted that significantly less of the Ala-containing peptide partitions into the bilayer phase, in what follows we will refer to the original 5/1 mole ratio for the sake of simplicity. Thin-layer chromatography of the samples before and after the NMR experiments showed that no appreciable degradation occurred during the course of the experiments.

All of the NMR spectroscopy was carried out on a Bruker MSL 300 wide-bore spectrometer with a 7.05-T magnet. A Novex (Gaithersburg, MD) 1-kW power amplifier and Bruker solenoidal coil probe afforded deuterium 90° pulse widths of approximately 3.5 μs. ^{2}H NMR measurements were made by using the quadrupole echo pulse sequence (Davis et al., 1976) with a pulse spacing of 25 μs, quadrature detection and a CYCLOPS sequence to minimize artifacts, a sweep width of at least 1.25 MHz, and a recycle time of 500 ms. The receiver was carefully adjusted so that signal occurred in only one channel. The out-of-phase channel containing only noise was zeroed giving symmetric spectra upon Fourier transformation and an increase in signal/noise by a factor of $\sqrt{2}$ (Davis, 1983).

Spectral "de-Paking" (Sternin et al., 1983; Bloom et al., 1981) and moment analyses were performed on a DEC LSI-11/23 microcomputer. We found that using 2048 spectral points the de-Paking algorithm required 3–4 iterations at ~1 h/iteration before the procedure converged. The de-Paking procedure is a deconvolution in which the Pake doublet powder pattern contribution to the line shape is extracted from the spectrum, leaving essentially the "oriented" spectrum that would have been obtained had all bilayers been situated parallel to the static magnetic field. In a single-component powder pattern spectrum, $\Delta\nu_q$ is the separation between the two maxima (perpendicular orientation), while in the de-Paked version there is a single peak whose offset from the origin is $\Delta\nu_q$. Spectral moment analysis as applied to ^{2}H NMR spectra is considered in detail by Davis (1983). The nth moment, M_n, of $f(\omega)$ is

$$M_n = \int_0^\infty d\omega\, \omega^n f(\omega) / \int_0^\infty d\omega\, f(\omega) \qquad (1)$$

Only positive frequencies are considered in order to obtain nonzero even *and* odd moments. The first moment is proportional to the average quadrupole splitting ($\langle\Delta\nu_q\rangle$), and the second moment gives the mean square quadrupole splitting

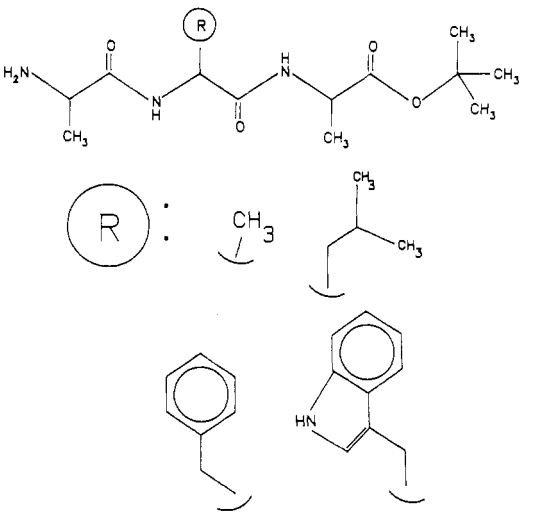

FIGURE 1: Structural formulas for the peptides used in this work.

$[\langle(\Delta\nu_q)^2\rangle]$. A simple combination of M_1 and M_2 gives the relative mean-squared width of the distribution of quadrupole splittings (Δ_2):

$$\Delta_2 = \frac{\langle(\Delta\nu_q)^2\rangle - \langle\Delta\nu_q\rangle^2}{\langle\Delta\nu_q\rangle^2} = \frac{M_2}{1.35M_1^2} - 1 \qquad (2)$$

The order parameter for the carbon–deuterium bond (S_{CD}) is proportional to $\Delta\nu_q$:

$$\Delta\nu_q = (3/4)(e^2qQ/h)S_{CD} \qquad (3)$$

where e^2qQ/h = 167 kHz (Burnett & Muller, 1971). The various moments and their combinations provide information about the degree and type of orientational averaging in multiple-labeled systems:

$$M_1 \propto \langle S_{CD}\rangle \qquad (4)$$

$$\Delta_2 \propto \frac{\langle S_{CD}^2\rangle - \langle S_{CD}\rangle^2}{\langle S_{CD}\rangle^2} \qquad (5)$$

Spin–lattice relaxation times were measured by using the inversion–recovery pulse sequence [π–τ–(π/2)–acquire] in which the quadrupole echo pulse sequence was substituted for the $\pi/2$ observation pulse. For the ^{2}H-labeled lipids, peak amplitudes were taken from the de-Paked spectra (Williams et al., 1985). For the ^{2}H-labeled peptide, intensities were measured at the "90° orientation" peaks in the powder spectra. A three-parameter nonlinear least-squares analysis using 12–15 different time points was employed to determine T_1 from the experimental data (Levy & Peat, 1975). Errors in all T_1 measurements are ~10%.

RESULTS

The Ala-X-Ala-*O-tert*-butyl peptides used in this study are shown in Figure 1. ^{2}H NMR powder and de-Paked spectra of bilayers formed from acyl chain perdeuteriated DMPC ([$^2H_{54}$]DMPC) with and without the addition of peptide are shown in Figures 2 and 3. All samples were prepared at a lipid/peptide mole ratio of 5/1; spectra were recorded at 30 °C. Because the spectra are symmetric, only half of each de-Paked spectrum is shown. The de-Paked spectra are scaled so that the quadrupole splitting ($\Delta\nu_q$) of the peaks can be read off of the abscissa as their offset from the origin. Peptide-induced changes in the powder spectra are noticeable as relatively small alterations in the overall shape of the overlapping

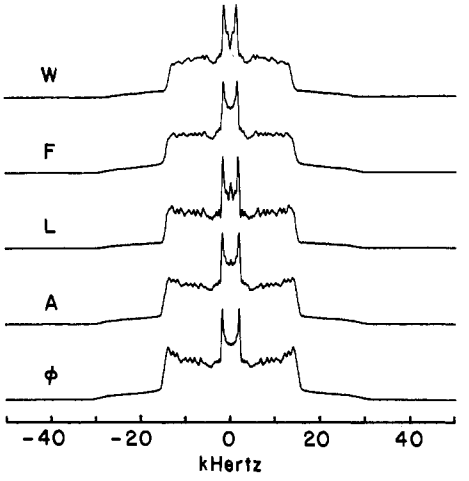

FIGURE 2: ^2H NMR spectra of multilamellar samples of [$^2H_{54}$]DMPC without (ϕ) and with the addition of peptides of the form A-X-A-*O-tert*-butyl, where X = Trp (W), Phe (F), Leu (L), or Ala (A). The samples contain a lipid/peptide mole ratio of 5/1. Spectra were recorded at 30 °C.

fatty acid methylene powder patterns. These alterations are qualitatively more conspicuous in the de-Paked versions of the spectra. Addition of the X = Ala peptide causes essentially no change in the spectra, while a significant decrease in $\Delta\nu_q$ for all of the peaks is observed upon the addition of the larger peptides (see top portion of Figure 3). As the size of the peptide central residue is increased from Ala to Leu to Phe to Trp, the $\Delta\nu_q$'s for corresponding peaks in the de-Paked lipid spectra become progressively smaller and the resonances that overlap in the order parameter "plateau region" at large $\Delta\nu_q$ in the pure bilayer spectra begin to spread out.

Figure 4 shows the effect of temperature changes on the de-Paked spectra of pure [$^2H_{54}$]DMPC bilayers and bilayers with the Trp- and Leu-containing peptides. Spectra obtained after incorporation of the Phe and Ala peptides are similar to those observed with the Trp and Leu peptide containing bilayers, respectively (data not shown). The broad, rather featureless spectra seen at 15 °C in Figure 4A,B are indicative of gel-phase lipids. The 15 °C spectra for the Trp peptide containing bilayer (Figure 4C) has both broad and narrow components. Moreover, the 20 °C spectrum in Figure 4C has distinctly narrower lines than those in the pure bilayer or the bilayer containing the Leu peptide. At higher temperatures all the spectra exhibit relatively sharp lines and the quadrupole splittings decrease monotonically with increasing temperature. The moments of spectra like those in Figure 4 provide a quantitative assessment of the distribution of order parameters found in the bilayer. Values for M_1 and Δ_2 at two temperatures (15 and 25 °C) for each of the bilayer systems examined are shown in Figure 5. Both above and below the bilayer phase transition temperature there is a decrease in M_1 (open symbols) with increase in the size of the peptide central residue, although the effect is much more pronounced at the lower temperature. This implies a similar decrease in the average order of the system. The relative mean-squared width of the bilayer order parameter distribution shows the opposite trend: Δ_2 increases with increasing peptide central residue size (solid symbols). The Ala, Leu, and Phe peptides cause small changes in Δ_2, while there is a dramatic decrease in Δ_2 for the bilayer at 15 °C containing the Trp peptide.

In order to access the influence of these small hydrophobic peptides on the dynamical behavior of the bilayer, we have measured lipid acyl chain ^2H spin–lattice relaxation rates. Relaxation rates for the resolved methylene resonances in

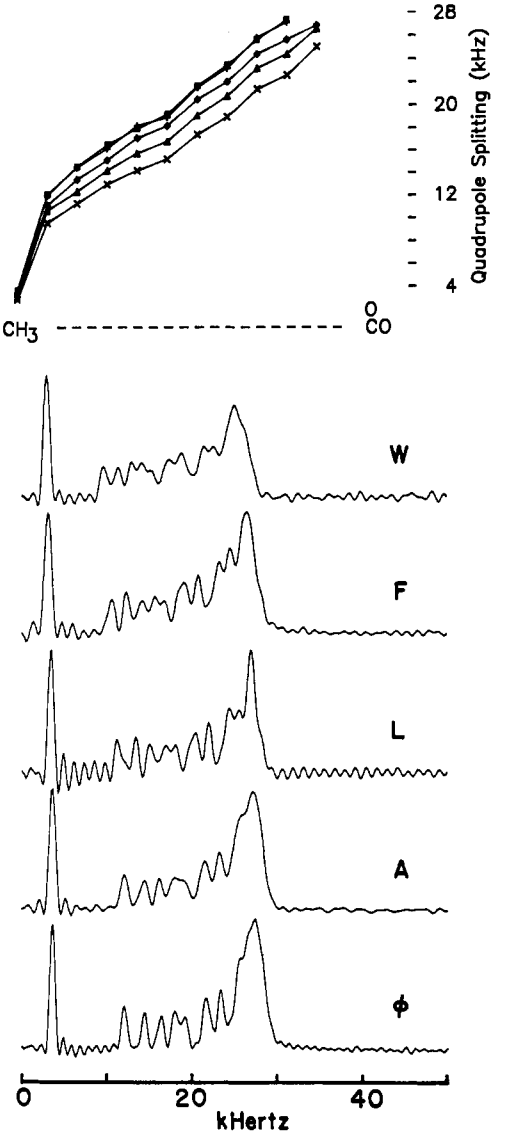

FIGURE 3: Upper graph shows quadrupole splittings for the well-resolved resonances seen in the de-Paked ^2H NMR spectra of the lipid/peptide mixtures shown in the lower portion of the figure. Pure DMPC (□) and DMPC/A-A-A-*O-tert*-butyl mixture (+) points are coincident, while the mixtures with A-L-A-*O-tert*-butyl (◇), A-F-A-*O-tert*-butyl (△), and A-W-A-*O-tert*-butyl (×) have decreasing quadrupolar splittings. Due to the difficulty of assigning the resonances to specific methylene units (see Discussion), we indicate only that the methyl resonance occurs at smallest $\Delta\nu_q$ and, in general, those nearer the carboxyl end have larger $\Delta\nu_q$ values. Only the right half of the symmetric de-Paked spectra are shown. Symbols are as in Figure 2 where the original spectra are shown.

de-Paked spectra of pure [$^2H_{54}$]DMPC bilayers and bilayers with the addition of each of the peptides were measured at 30 °C. In liquid crystal systems, under certain circumstances, $1/T_1$ should be proportional to S_{CD}^2 (Doane & Johnson, 1970; Brown, 1982). The relaxation rates are shown in Figure 6 plotted against the squared order parameters for the C–$^2H_2$ units calculated according to eq 3. In all five cases the relaxation rates are linearly related to S_{CD}^2. Linear least-square fits are shown as solid lines in Figure 6. The ordinate intercepts of the fits all fall within two standard deviations of one another and are thus not differentiated by these data. The average intercept is 2.6 ± 3 s^{-1}. Conversely, as can be seen from Figure 6, the slopes for all of the peptide-containing bilayers are significantly larger than that found for the pure bilayer. The values for the slopes are as follows: pure bilayer, 591 ± 61; bilayer plus A-A-A-*O-tert*-butyl, 1288 ± 120; bi-

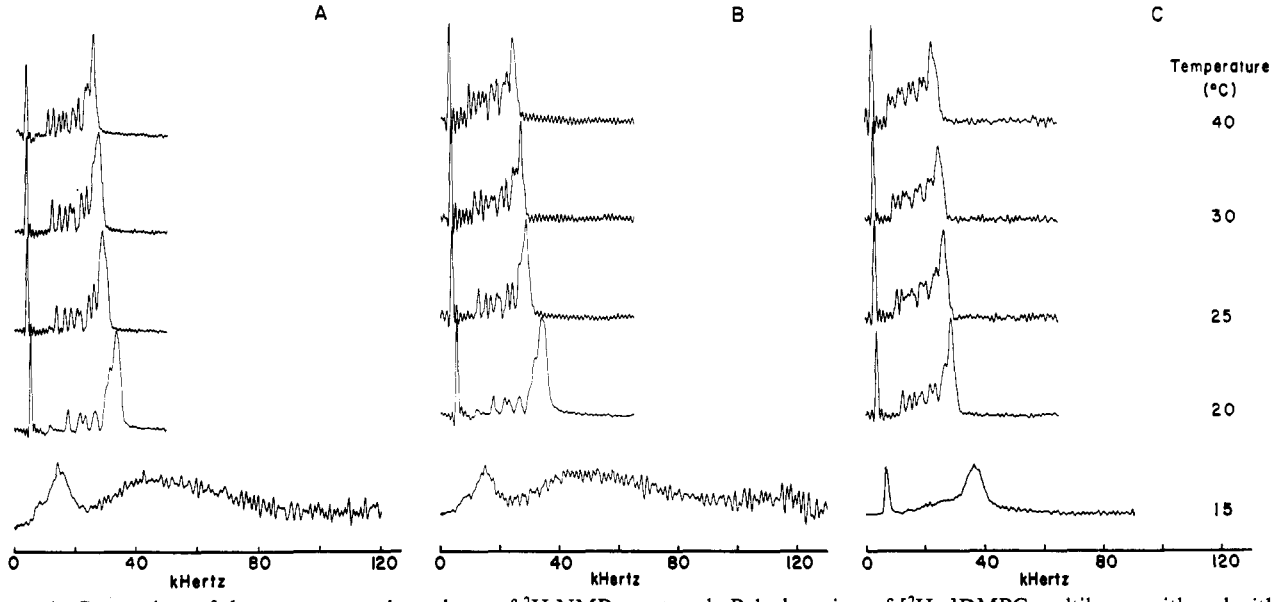

FIGURE 4: Comparison of the temperature dependence of ^2H NMR spectra, de-Paked version, of [$^2H_{54}$]DMPC multilayers with and without addition of peptide: (A) no addition; (B) plus Leu-containing peptide; (C) plus Trp-containing peptide. Temperature decreases from top to bottom spectra as follows: 40, 30, 25, 20, and 15 °C.

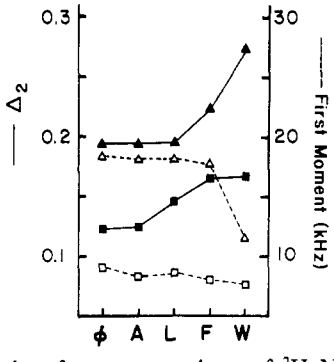

FIGURE 5: Results of moment analyses of ^2H NMR spectra of multilamellar samples of [$^2H_{54}$]DMPC alone (ϕ) and with the addition of the indicated peptides. Squares represent 25 °C data and triangles 15 °C data. Open symbols are the first "half-moments" of the spectra which are proportional to $\langle S_{CD} \rangle$. Filled symbols represent $\Delta_2 = [M_2/(1.35M_1^2)] - 1 = [\langle S_{CD}^2 \rangle - \langle S_{CD} \rangle^2]/\langle S_{CD} \rangle^2$, where M_i is the ith half-moment. Symbols are essentially the size of the errors in M_1 and Δ_2.

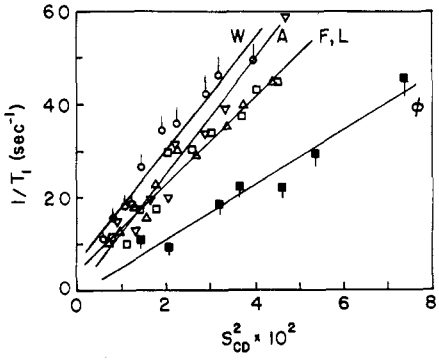

FIGURE 6: Plots of spin–lattice relaxation rates $1/T_1(i)$ vs. $|S_{CD}(i)|^2$ for multilamellar samples of [$^2H_{54}$]DMPC alone (ϕ) and with the addition of the indicated peptides. Symbols correspond to samples as follows: ϕ (■), A (▽), L (△), F (□), and W (○). Linear least-squares fits to the respective data sets are shown. The fits to the Phe and Leu data sets are coincident. Relaxation rates were derived from de-Paked spectra. Error in T_1 measurements of ~10% are noted for the ϕ and W data sets. Uncertainty in the other data points is similar.

layer plus A-L-A-*O-tert*-butyl, 956 ± 85; bilayer plus A-F-A-*O-tert*-butyl, 954 ± 60; bilayer plus A-W-A-*O-tert*-butyl, 1217 ± 92.

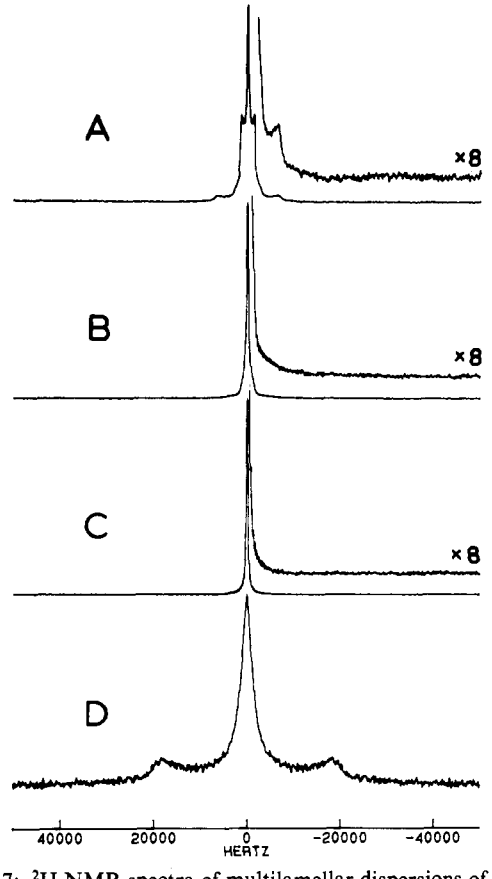

FIGURE 7: ^2H NMR spectra of multilamellar dispersions of DMPC with 20 mol % Ala-[$^2H_4$]Ala-Ala-*O-tert*-butyl obtained at temperatures of (A) 25, (B) 20, (C) 0, and (C) −20 °C. The ^2H NMR spectrum of polycrystalline powder peptide (not shown) exhibits the same 38-kHz quadrupolar splitting observed in spectrum D.

Figure 7 shows ^2H NMR spectra of Ala-[$^2H_4$]Ala-Ala-*O-tert*-butyl in DMPC bilayers at a lipid/peptide mole ratio of 5/1. The deuteriated Ala group spectra show a rather complicated temperature dependence. In the liquid-crystalline bilayer at 25 °C the spectrum exhibits three overlapping components: an isotropic peak and two powder patterns with $\Delta\nu_q$ = 3.8 and 13.5 kHz. At 20 °C, just below the bilayer phase transition, the spectrum is dominated by a narrow iso-

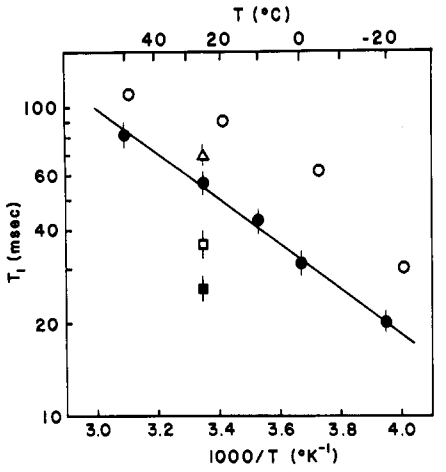

FIGURE 8: Spin–lattice relaxation times for deuteriated Ala residues in various environments: polycrystalline Ala·HCl (O) data from Keniry et al. (1984), polycrystalline Ala-[$^2H_4$]Ala-Ala-*O-tert*-butyl (●), the isotropic (□) and major powder pattern (■) components observed in spectrum A of Figure 7, and the C–$^2H_3$ resonance of the peptide in aqueous solution (△). Bars denote ±10% error in T_1 measurements.

tropic component with a very broad base, suggesting an underlying anisotropic component with $\Delta\nu_q < 2$ kHz (Figure 7B). Lowering the temperature to 0 °C brings about a loss of virtually all the anisotropic portion of the spectrum, and a single Lorentzian line is observed in Figure 7C. Upon further lowering of the temperature to −20 °C, the line width of the isotropic component increases dramatically and an anisotropic component with $\Delta\nu_q = 38$ kHz is observed (Figure 7D). In polycrystalline powders of the peptide we observe a single powder pattern with a quadrupole splitting of 38 kHz. Similar spectra have been obtained by Keniry et al. (1984) for a number of polycrystalline methyl-deuteriated amino acids. These workers also measured spin–lattice relaxation times and computed correlation times for methyl rotation as a function of temperature. In Figure 8 we compare the spin–lattice relaxation times for polycrystalline L-alanine (hydrochloride form), polycrystalline Ala-[$^2H_4$]Ala-Ala-*O-tert*-butyl, and the peptide in DMPC liposomes at a lipid/peptide mole ratio of 5/1. A similar temperature dependence is observed for the two polycrystalline species, although the T_1's for the peptide Ala methyl group are consistently shorter than those of the amino acid. The triangle in Figure 8 shows the T_1 for the methyl group of the deuteriated peptide in aqueous solution. The squares in Figure 8 show T_1 values for the isotropic peak and the major powder pattern observed in the 25 °C spectra of the lipid/peptide mixture (Figure 7A). Both are significantly less than that found for the polycrystalline powder.

DISCUSSION

Using acyl chain perdeuteriated lipids and the spectral de-Paking procedure, we have obtained ^2H NMR spectra of a variety of lipid/peptide mixtures as seen in Figures 3 and 4. Although the assignment of each of the resonance peaks to specific methylene groups on either of the acyl chains is ambiguous, comparisons with spectra of specifically deuteriated lipids (Oldfield et al., 1978) and single acyl chain perdeuteriated lipids (Paddy et al., 1985) allow us to make some unequivocal assignments. The peak at smallest $\Delta\nu_q$ (~3.7 kHz) arises from the terminal methyl groups, while the broad peak with the largest $\Delta\nu_q$ (~28 kHz) arises from about five methylenes near the bilayer surface with nearly the same order parameter (the so-called plateau region). Some of the well-resolved peaks at intermediate $\Delta\nu_q$ come from deuterons at the C-2 position which have anomalously small $\Delta\nu_q$ values (Oldfield et al., 1978), while the remainder come from methylene groups near the center of the bilayer. In general, the larger the splitting the further the methylene group is from the terminal methyl group.

As seen from the graph and spectra in Figure 3, there is an observable decrease in bilayer order upon the introduction of the hydrophobic tripeptides. The largest effect is seen in the methylene plateau region where the $\Delta\nu_q$ values decrease by about 5 kHz in the presence of peptide. Similar decreases in $\Delta\nu_q$ are seen for the intermediate methylene positions, and a small decrease is even seen in the quadrupole splitting of the terminal methyl group. There is more apparent disruption of the bilayer order as the peptide central residue side chain becomes larger; some of the plateau region methylene units shift to smaller $\Delta\nu_q$ values and become distinct peaks in the de-Paked spectra (see the 20 and 25 °C spectra in Figure 4). These observations indicate that the introduction of peptide produces a disordering along the entire length of the lipid acyl chains.

Previous calorimetric work on these lipid/peptide mixtures indicated that the Trp- and Phe-containing peptides induce a phase separation in the plane of the bilayer, while the peptides with small side chains act as simple impurities (Jacobs & White, 1986). Taking into account the several degree lower phase transition temperature of the perdeuteriated vs. the protonated lipid, the temperature dependencies of the ^2H NMR spectra of the mixture are consistent with the phase diagrams proposed for these systems. Significant increases in line widths and quadrupolar splittings on going from 25 to 20 °C in pure bilayers and bilayers with the Leu peptide (Figure 4A,B) indicate that both systems begin to enter the gel phase at ~20 °C. At 15 °C the ^2H NMR spectra with and without the Leu peptide exhibit the broad lines characteristic of gel-phase lipids. Similar behavior was observed for the Ala peptide (data not shown). Qualitatively different behavior was observed for bilayers containing the Trp peptide: resonances in the 20 °C spectrum are still quite sharp, while the resonances in the 15 °C spectrum have line widths intermediate between those observed for liquid-crystalline and gel-phase lipids. Similar, but less pronounced, results were obtained for mixtures of the Phe peptide (data not shown). Thus the broad endotherms seen in the DSC thermograms are manifested in the ^2H NMR spectra as multiple overlapping line shapes. The same phenomenon has been observed in mixtures of simple lipids (Jacobs & Oldfield, 1979) and mixtures of relatively large hydrophobic peptides with lipid bilayers (Davis et al., 1983).

We can make more detailed statements about the effect of the peptides on the average bilayer order and the order parameter distribution across the bilayer using the results of the spectral moment analyses shown in Figure 5. The open symbols show that at both high and low temperatures the addition of peptide causes a decrease in the average acyl chain order. The change is small for the Ala- and Leu-containing peptides and progressively larger for the Phe- and Trp-containing peptides. The largest decrease in $\langle S_{CD} \rangle$ is seen in the low-temperature curve (Figure 6, open triangles) where M_1 for the Trp peptide mixture approaches that of the 25 °C pure DMPC bilayer. This is not surprising because at 15 °C and 20 mol % A-W-A-*O-tert*-butyl the bilayer is a mixture of gel and liquid-crystalline phases (vide supra). The solid lines and symbols in Figure 5 show that the relative width of the order parameter distribution increases upon the addition of peptide. If the methylene units in the order parameter plateau region near the bilayer surface were disordered more than those with smaller order parameters near the bilayer center, then we

would expect a decrease in the relative mean-squared width of the distribution of order parameters, Δ_2. The opposite effect is observed, indicating that the perturbations caused by the peptides are at least as large in the bilayer interior as at the bilayer surface. Moreover, increasing the size of the peptide central residue causes a concomitant increase in Δ_2. This implies, again, that the extent of bilayer perturbation is directly related to the size of the peptide. Similar trends in M_1 and Δ_2 have been observed for bilayers containing rhodopsin (Bienvenue et al., 1982; Deese et al., 1981) where small decreases in M_1 and large increases in Δ_2 accompany incorporation of the protein into the bilayer membrane.

Acyl chain methylene ^2H NMR spin–lattice relaxation rates have been observed to follow a square-law dependence on orientational order (Doane & Johnson, 1970; Ukleja et al., 1976; Brown, 1982; Paddy et al., 1985). The data shown in Figure 6 for pure DMPC bilayers are in good agreement with those of Williams et al. (1985), especially considering the different magnetic fields used. After the addition of peptide the plots of $1/T_1$ vs. S_{CD}^2 are still linear but differ significantly from the pure lipid plot. Although the relaxation rates measured in the presence of peptide were all faster than in their absence, there are some differences among the peptide data sets also. To interpret data of this type in terms of the microscopic behavior of the lipids, one must make assumptions concerning the types of motions that modulate the relaxation processes. Most models for relaxation in these bilayer systems divide the motions into two classes: fast and slow relative to the resonance frequency (Bocian & Chan 1978; Brown, 1982; Marqusee et al., 1984). Within the context of the models of Brown (1982) and Marqusee et al. (1984), the ordinate intercepts of the lines in Figure 7 are determined by the correlation time for the fast motions, while the slow motions influence the slopes. Considering the time scales involved, the slow motions are attributed to collective modes within the bilayer (e.g., director fluctuations and/or bilayer deformations) and the fast motions include chiefly gauche–trans isomerization. These theories further interpret increases in the slope of $1/T_1$ vs. S_{CD}^2 as being related to a decrease in the "microviscosity" and/or "elastic modulus" of the bilayer. In contrast to this interpretation, work aimed at developing generalized model-independent theories of relaxation time measurements (Meier et al., 1986; Lipari & Szabo, 1982a,b) implies that collective modes do not contribute significantly to T_1 relaxation times in lipid bilayer systems. In this case, the changes in the acyl chain relaxation times brought about by the peptides must arise from modulation of fast motions, such as chain fluctuations and/or rotation.

Cornell et al. (1982) have taken advantage of the fact that $T_{1\rho}$ is also sensitive to slow motions (Slichter, 1978). They noted the sensitivity of proton-enhanced ^{13}C NMR measurements of the lipid methylene $T_{1\rho}$ to the presence of gramicidin A^+. $T_{1\rho}$ in the presence of gramicidin A^+ was reduced to 26 ms from the pure bilayer value of 85 ms, although no change in T_1 was observed. Applying the "fast/slow motion" model to the data in Figure 6 yields essentially the same conclusions as Cornell et al. (1982) draw from their T_1 and $T_{1\rho}$ measurements: (1) the fast local chain motions are largely unaffected by the presence of peptide, and (2) the incorporation of peptide significantly increases the amplitude of the slow collective class of acyl chain motions. For the tripeptides, the extent of the effect is somewhat peptide dependent but does not vary monotonically with the size of the central residue.

Additional insight into the alterations of the lipid acyl chain dynamic behavior caused by these small hydrophobic peptides may be gained by comparing the plots in Figure 6 with similar data obtained for pure lipid bilayers composed of different types of lipids. Williams et al. (1985) found that plots of $1/T_1$ vs. S_{CD}^2 for DLPC, DMPC, and DPPC (all acyl chain perdeuteriated) are superimposable to within experimental error. Paddy et al. (1985) examined phosphatidylcholines in which perdeuteriated palmitic acid was esterified to the glycerol *sn*-1 position and either palmitic (16:0), docosahexenoic (22:6), or palmitoleic (16:1) acid was esterified to the *sn*-2 position. The slopes of $1/T_1$ vs. S_{CD}^2 for both of the unsaturated bilayers are significantly larger than that of the fully saturated bilayer. Surprisingly, the 16:1-containing lipids exhibited a larger slope than the 22:6-containing lipid bilayers. The slopes for the DMPC bilayers with the Ala- and Trp-containing peptides ($\sim 1250 S_{CD}^{-2}$ s^{-1}) were quite similar to the slope obtained for the 22:6-containing lipids ($1340 S_{CD}^{-2}$ s^{-1}), while the slopes for DMPC bilayers with the Leu- and Phe-containing peptides ($\sim 950 S_{CD}^{-2}$ s^{-1}) are somewhat less, although still larger than the slope of the pure DMPC bilayer plot ($\sim 600 S_{CD}^{-2}$ s^{-1}). The intercepts for both of the unsaturated lipid bilayers (13.7 s^{-1} for the 16:1 species and 11.6 s^{-1} for the 22:6 species) are larger than the intercepts for the peptide/bilayer mixtures whose intercepts are indistinguishable from the pure lipid system intercepts (~ 3 s^{-1}). Thus the magnitude of the alterations in the lipid motions caused by the hydrophobic peptides is quite similar to that caused by changing the *sn*-2 position from a 16:0 to a 22:6 fatty acid. In contrast, no measurable change in the fast motional regime is induced by the addition of peptide, while fatty acid alteration produces considerable change. Exactly what this tells us about the details of the packing of the lipid/peptide mixtures is unclear, because little is known about the packing of polyunsaturated lipids and because mixed-chain lipids display complex behavior (McIntosh et al., 1984; Mason et al., 1981). It is clear, however, that the peptides are quite effective modulators of the slow motions. At 20 mol % they produce the same change as when half the lipid acyl chains are substituted with the 22:6 fatty acid.

There is a large body of experimental and theoretical work on methyl group reorientation (Torchia & Szabo, 1982; Batchelder et al., 1982; Keniry et al., 1984). The peptides used in this study are intermediate in structural complexity between the simple amino acids and very complex membrane proteins examined by Keniry et al. (1984). In a recent study using a protected dipeptide (Boc-Leu-Phe-OMe selectively labeled at a number of sites) in lipid bilayers, Mueller et al. (1986) observed a complex dependence of the peptide ^2H NMR spectra on temperature. Many of the spectra of this peptide in DMPC bilayers had unusual line shapes in the sense that they did not fit either a rapid rotation or a jump reorientation model. The ^2H NMR spectra of Ala-[$^2H_4$]Ala-Ala-*O*-*tert*-butyl shown in Figure 7 reveal that mixtures of this peptide in DMPC liposomes also exhibit complex behavior. In the 25 °C spectrum the two powder patterns have roughly the appropriate intensities to originate from the β-C^2H_3 and α-C^2H groups. Relaxation time measurements (vide infra) indicate that the isotropic resonance does not arise from "free" peptide in the aqueous phase, although it may come from peptide loosely associated at the water/bilayer interface. If the Ala peptide bilayer partitioning decreases with decreasing temperature, we expect decreasing amounts of the powder pattern component (bound peptide) and increasing intensity from the isotropic component (relatively "free" peptide) in the peptide spectra as the temperature is lowered. At 20 and 0 °C the bilayer is in the gel phase and the peptide spectra are domi-

nated by the isotropic component, whereas in the lipid-crystalline phase at 25 °C most of the spectral intensity is in the order powder pattern component. The implication is that as the bilayer passes into the gel phase, the peptide becomes disassociated. The 38-kHz quadrupole splitting observed in the −20 °C spectrum is characteristic of methyl groups undergoing fast reorientation ($>10^7$ s^{-1}), indicating that other types of motion have been frozen out at this low temperature.

Deuterium relaxation times can be used to calculate activation energies and rotational correlation times by using methods outlined by Torchia and Szabo (1982) and Keniry et al. (1984) assuming a three-site jump model for the methyl reorientation. Figure 8 shows that the temperature dependence of the ^2H spin–lattice relaxation times in polycrystalline Ala-[$^2H_4$]Ala-Ala-*O-tert*-butyl is essentially the same as that observed for polycrystalline alanine hydrochloride [open circles, data from Keniry et al. (1984)]. The absolute values for the peptide relaxation times are somewhat less than those observed for the amino acid. Thus, the activation energies for methyl rotation in the polycrystalline peptide and amino acid are not significantly different, while the rotational correlation time is longer for the peptide: 31 ps for Ala·HCl vs. 108 ps for the peptide. The correlation time for the zwitterionic form of Ala is much longer (~800 ps; Keniry et al., 1984), indicating a significantly larger barrier to rotation in this system than in either the HCl form or the peptide.

Spin–lattice relaxation times for the deuteriated peptide in DMPC bilayers and in aqueous solution at 25 °C are also shown in Figure 8. The isotropic line shapes and greatly reduced quadrupole splittings seen in Figure 7 indicate that motions other than simple methyl rotation are important in these systems. This greatly complicates the analysis of the relaxation times. Qualitatively, one might expect the decreasing degree of constraint on molecular motion upon going from the crystalline peptide to bilayer-incorporated peptide to aqueous peptide solutions to be reflected in increasing values of T_1 (i.e., in the fast motion limit $1/T_1 \propto \tau_c$). In fact, the maximum T_1 is found for the peptide in solution. However, in the peptide/DMPC mixture both the isotropic peak and the 3.8-kHz powder pattern have T_1 values significantly less than the crystalline peptide. Thus, the simple-minded notion of constraints being lifted is incomplete. The additional types and time scales of motion (over and above methyl rotation) that the peptide is undergoing in the presence of lipid bilayer membranes afford relaxation pathways not present in either the crystal or aqueous solution.

The present and previous (Jacobs & White, 1986) studies of the tripeptide/lipid mixtures have not directly addressed the important question of the location of the peptides in the bilayer. Knowledge of the specific location is necessary before we can decide among several possible interpretations of the lipid and peptide behavior noted in these studies. We consider three possibilities: (1) The peptides are adsorbed at the lipid/water interface, (2) the peptide amino terminus is located near the interface with the remainder of the molecule extending into hydrocarbon core, and (3) the peptide is immersed in the bilayer hydrocarbon core. Possibility 3 is unlikely, because it would involve transferring the *charged* amino terminus (all these experiments were performed at pH 7) completely out of the aqueous phase into the bilayer interior. Possibility 2 would place the central and carboxy-terminal peptide residues and the *tert*-butyl group within the acyl chain matrix and thus account directly for the Trp fluorescence enhancement found in the A-W-A-*O-tert*-butyl/DMPC mixtures (Jacobs & White, 1986), the general increase in lipid acyl chain disorder produced by the peptides, the correlation between the extent of lipid disorder and peptide size, and the apparent ejection of A-A-A-*O-tert*-butyl from the gel-phase bilayer. Tetracaine hydrochloride appears to interact with DPPC bilayers in this way. ^2H NMR studies (Boulanger et al., 1980, 1981) indicate the presence of ordered tetracaine in tetracaine/bilayer mixtures and that the addition of the anesthetic leads to increased disorder along the whole length of the lipid acyl chain. Possibility 3, peptide adsorption to the bilayer surface, could also account for all these effects, but in a less direct manner. Changes in area per lipid molecule or alterations in lipid rotational and/or lateral diffusion could mediate these effects. The benzyl alcohol/DMPC mixture is an example of possibility 3 in which ^2H NMR studies show solute ordering (Pope et al., 1986) and a small amount of lipid chain disordering (Turner & Oldfield, 1979).

Conclusions

Perturbations in lipid order and dynamic features induced by the interaction of peptides of the form Ala-X-Ala-*O-tert*-butyl with the lipid bilayer extend the entire length of the lipid acyl chains. The quantitative features of the perturbations depend strongly on the identity of the central residue, the large peptides inducing more disorder than the smaller. Lipid acyl chain relaxation time measurements indicate that the peptides modulate the lipid motions in a complex fashion. Spectra and relaxation time measurements of a ^2H-labeled peptide show complex behavior in the bilayer. These general observations are in agreement with our previous calorimetric work on these lipid/peptide mixtures, with extensive studies employing membrane-spanning amphiphilic polypeptides (Davis et al., 1983), and with a study of mixtures of a small deuteriated peptide with different lipid bilayers (Mueller et al., 1986).

Acknowledgments

We thank April Diaz for synthesis of the peptides. We are especially grateful to Drs. Edward Sternin and Myer Bloom for a listing of their de-Paking routine and to Dr. Jay Edleman for assistance in implementing it on our computer system.

Registry No. A-W-A-*O-tert*-butyl, 100859-31-2; A-F-A-*O-tert*-butyl, 100859-30-1; A-L-A-*O-tert*-butyl, 92752-43-7; A-A-A-*O-tert*-butyl, 65356-57-2; DMPC, 18194-24-6.

References

Batchelder, L., Sullivan, C. E., Jelinski, L. W., & Torchia, D. A. (1982) *Proc. Natl. Acad. Sci. U.S.A. 79*, 386–389.

Bell, J. E. (1981) in *Spectroscopy in Biochemistry* (Bell J. E., Ed.) Vol. II, Chapter 4, CRC Press, Boca Raton, FL.

Bienvenue, A., Bloom, M., Davis, J. H., & DeVaux, P. F. (1982) *J. Biol. Chem. 257*, 3032–3038.

Bloom, M., Davis, J. H., & Valic, M. I. (1981) *Chem. Phys. Lett. 80*, 198–202.

Bloom, M., Holmes, K. T., Mountford, C. E., & Williams, P. G. (1986) *J. Magn. Reson. 69*, 73–91.

Bocian, D. F., & Chan, S. I. (1978) *Annu. Rev. Phys. Chem. 29*, 307–335.

Boulanger, Y., Schreier, S., & Smith, I. C. P. (1981) *Biochemistry 20*, 6824–6830.

Briggs, M. S., & Gierasch, L. M. (1984) *Biochemistry 23*, 3111–3114.

Brown, M. F. (1982) *J. Chem. Phys. 77*, 1576–1599.

Büldt, G., Gally, H. U., Seelig, J., & Zaccai, G. (1979) *J. Mol. Biol. 134*, 673–691.

Burnett, L. J., & Muller, B. H. (1971) *J. Chem. Phys. 55*, 5829–5831.

Cornell, B. A., Davenport, J. B., & Separovic, F. (1982) *Biochim. Biophys. Acta 689*, 337–345.
Davis, J. H. (1983) *Biochim. Biophys. Acta 737*, 117–171.
Davis, J. H., Jeffrey, K. R., Bloom, M., Valic, M. I., & Higgs, T. P. (1976) *Chem. Phys. Lett. 42*, 390–394.
Deese, A. J., Dratz, E. A., Dahlquist, F. W., & Paddy, M. R. (1981) *Biochemistry 20*, 6420–6427.
Doane, J. W. & Johnson, D. L. (1970) *Chem. Phys. Lett. 6*, 291–295.
Gremlich, H.-U., Fringeli, U.-P., & Schwyzer, R. (1983) *Biochemistry 22*, 4257–4264.
Huang, C.-H., & Charlton, J. P. (1972) *Biochemistry 11*, 735.
Huang, C.-H., & Thompson, T. E. (1974) *Methods Enzymol. 32*, 485–501.
Jacobs, R., & Oldfield, E. (1979) *Biochemistry 18*, 3280–3285.
Jacobs, R. E., & White, S. H. (1986) *Biochemistry 25*, 2605–2612.
Keniry, M. A., Kintanar, A., Smith, R. L., Gutowsky, H. S., & Oldfield, E. (1984) *Biochemistry 23*, 288–298.
King, G. I., & White, S. H. (1986) *Biophys. J. 49*, 1047–1054.
Lentz, B. R., Clubb, K. W., Alford, D. R., Hochli, M., & Meissner, G. (1985) *Biochemistry 24*, 433–442.
Levy, G. C., & Peat, I. R. (1975) *J. Magn. Reson. 18*, 500–521.
Lipari, G., & Szabo, A. (1982a) *J. Am. Chem. Soc. 104*, 4546–4559.
Lipari, G., & Szabo, A. (1982b) *J. Am. Chem. Soc. 104*, 4559–4570.
Marqusee, J. A., Warner, M., & Dill, K. A. (1984) *J. Chem. Phys. 81*, 6404.
Mason, J. T., Huang, C., & Biltonen, R. L. (1981) *Biochemistry 20*, 6086–6097.
McIntosh, T. J., Simon, S. A., Ellington, J. C., & Porter, N. A. (1984) *Biochemistry 23*, 4038–4044.
Meier, P., Ohmes, E., & Kothe, G. (1986) *J. Chem. Phys. 85*, 3598–3614.
Morrow, M. R., Huschilt, J. C., & Davis, J. H. (1985) *Biochemistry 24*, 5396–5406.
Mueller, L., Frey, M. H., Rockwell, A. L., Gierasch, L. M., & Opella, S. J. (1986) *Biochemistry 25*, 557–561.
Naik, V., & Krimm, S. (1986) *Biophys. J. 49*, 1147–1154.
Oldfield, E., Meadows, M., Rice, D., & Jacobs, R. (1978) *Biochemistry 17*, 2727–2739.
Paddy, M. R., Dahlquist, F. W., Dratz, E. A., & Deese, A. J. (1985) *Biochemistry 24*, 5988–5995.
Pope, J. M., Dubro, D., Doane, J. W., & Westerman, P. W. (1986) *J. Am. Chem. Soc. 108*, 5426–5433.
Rehorek, M., Dencher, N. A., & Heyn, M. P. (1985) *Biochemistry 24*, 5980–5988.
Rigell, C. W., de Saussure, C., & Freire, E. (1985) *Biochemistry 24*, 5638–5646.
Silvius, J. R. (1982) in *Lipid–Protein Interactions* (Jost, P. C., & Griffith, O. H., Eds.) Vol. II, Chapter 7, Wiley, New York.
Slichter, C. P. (1978) *Principles of Magnetic Resonance*, Chapter 6, Springer-Verlag, New York, NY.
Smith, R. L. & Oldfield, E. (1984) *Science (Washington, D.C.) 225*, 280–288.
Sternin, E., Bloom, M., & MacKay, M. L. (1983) *J. Magn. Reson. 55*, 274–282.
Surewicz, W. K., & Epand, R. M. (1985) *Biochemistry 24*, 3135–3144.
Torchia, D. A., & Szabo, A. (1982) *J. Magn. Reson. 49*, 107–121.
Ukleja, P., Pirs, J., & Doane, J. W. (1976) *Phys. Rev. A 14*, 414–423.
Wallace, B. A., Vetch, W. R., & Blout, E. R. (1981) *Biochemistry 20*, 5754–5760.
Williams, G. D., Beach, J. M., Dodd, S. W., & Brown, M. F. (1985) *J. Am. Chem. Soc. 107*, 6868–6873.
Wolber, P. K., & Hudson, B. S. (1982) *Biophys. J. 37*, 253–262.